

Characterisation of the Influence of Minor Elements on Microstructure Variations in a Secondary Cast Aluminium Piston Alloy

Thomas O. Mbuya¹, Ian Sinclair¹, Bruno R. Mose², Stephen M. Maranga² and Philippa A. S. Reed¹

¹Engineering Materials Group, School of Engineering Sciences, SO17 1BJ, University of Southampton, UK.

²Department of Mechanical Engineering, Jomo Kenyatta University of Agriculture & Technology, P.O. Box 62000 (00200), Nairobi, Kenya.

The influence of minor elements (Sr, Sb, Mn, Cr and Al-5Ti-B) on the microstructure and porosity in a secondary piston Al-Si alloy was investigated using SEM-EDX and micro-focus computed tomography (μ CT) tools. Porosity and intermetallic characteristics were measured in the 3D μ CT volumes as well as on 2D SEM images. The intermetallics occurring were identified using EDX and by cross-referencing with previous work. The volume fraction (V_f) of intermetallics increased with minor element additions except when 0.2%Sb was added. Sb decreased V_f but increased β -Al₅FeSi particles in the alloy. This effect was cancelled with addition of 0.2%Sb+0.53%Mn. Porosity increased with all additions except for 1%Cr, which resulted in fine compact intermetallics and reduced porosity. Addition of 0.53%Mn and 0.3%Mn+0.2%Cr also resulted in compact phases and low porosity. Porosity was highest in the Sr-modified alloys with 0.02%Sr giving higher porosity than 0.05%Sr. However, porosity reduced in the 0.02%Sr alloy with 0.53%Mn addition while addition of 0.53%Mn+0.05%Sr significantly increased the level of porosity and intermetallics.

Keywords: Al-Si Alloy, Eutectic Si modification, Cast Aluminium Recycling, Fe-rich Intermetallics.

1. Introduction

Secondary Al-Si alloys are now increasingly applied in automotive components such as cylinder heads because of their relatively low cost and associated environmental benefits. These alloys however have higher impurity levels that influence their castability, microstructure and mechanical properties. Iron is a common impurity that leads to the formation of various intermetallic phases that deteriorate the castability and mechanical performance of these alloys. The most detrimental phase is often identified as β -Al₅FeSi because of its plate-like morphology. Addition of elements such as Mn, Cr, Be, Co, and Sr lead to formation of other phases with less harmful morphologies [1,2]. Mn is widely used at an Fe:Mn ratio of 2 although alternative levels have also been proposed [1,3]. Cr is less popular due to claims that it tends to form sludge [1]. However, others have shown that addition of Cr alone or Cr and Mn can be more effective than Mn alone [4,5]. Sr and Sb are often added to modify eutectic Si [6] but Sr has also been shown to suppress β -phase formation [7]. It is also reported to lead to the fragmentation of the β -phase [8]. Addition of Ti-based grain refiners have also been reported to coarsen the β -phases [1,8].

These observations have however mainly been reported in simpler commercial alloys such as A356 and 319-type alloys. Piston alloys have a higher alloying content leading to the formation of a complex network of intermetallics. Some of the unique phases in piston alloys include Al₃Ni, Al₉FeNi, Al₇Cu₄Ni and Al₃(Cu,Ni)₂ due to their high Ni level [9-11]. The β -phase is not common in these alloys although it does occasionally appear in some alloys [9-12]. The phases that ultimately occur, depend on the alloy chemistry and cooling rate. The effect of these phases on the castability of piston alloys is not well understood. For reliable application of recycled piston alloys, it is necessary to have a clear understanding of the effect of minor elements that may be inadvertently present as impurities. This paper reports the effect of various minor elements on the microstructure and porosity characteristics of a secondary piston alloy with a high Fe level (1.08%).

2. Experimental Method

The alloy investigated was obtained from piston scrap and its chemistry determined as 10.6%Si, 1.36%Cu, 1.08%Ni, 0.78%Mg, 1.06%Fe, 0.08%Mn, 0.03%Cr, 0.06%Ti, 0.02%Sn, 0.09%Zn, 0.04%K. It is equivalent to the AE413 alloy recently investigated by Daykin [9]. Eleven variants of this alloy were obtained by adjusting the level of minor elements as follows: P (no addition), P2Sr (0.02%Sr), P5Sr (0.05%Sr), PSb (0.2%Sb), PMn (0.53%Mn), PMnCr (0.3%Mn+0.2%Cr), P2SrGr (0.02%Sr+0.28%Al-5Ti-1B), P2SrMn (0.02%Sr+0.53%Mn), P5SrMn (0.05%Sr+0.53%Mn) and PCr (1.06%Cr).

Bar castings were produced from these alloys and specimens for microstructure analysis sectioned. These were polished to OPS finish and observed using a JEOL JSM 6500F SEM microscope with EDX capability. Furthermore, $\sim 2 \times 2 \times 20$ mm samples were scanned using an X-tek CT 160Xi micro-focus Computed Tomography (μ CT) scanner at a filament current of 68 μ A and an accelerating voltage of 68 kV using a molybdenum target. No filter was used and the CMOS detector used a frame rate of 2 fps and a digital gain of 1. The reconstructed volumes were analysed using VG Studio Max 2.0 and ImageJ to characterise the volume fraction (V_f) of intermetallics and porosity. The μ CT data was also used to obtain the size and shape (α -aspect ratio) distribution of porosity. The resolution of the μ CT images was ~ 5 μ m and not adequate to analyse the size distribution of intermetallics. Instead, at least 10 backscattered (BEI) SEM images (at X150) were analysed for each alloy using ImageJ. The dendrite arm spacing (DAS) was measured using ImageJ and found to be 28 μ m. This corresponds to a cooling rate of $\sim 3.4^\circ\text{C/s}$ as computed using the expression $\lambda = CR^{-\phi}$ ($C=45.7$, $\phi=0.4$ and $\lambda=28$ μ m) [4].

3. Results and Discussion

The as-cast microstructure of the base alloy is shown in Fig. 1 in which the various phases observed are identified. The Mg_2Si phase was also observed. The Al_9FeNi phase was frequently observed as thin or thick plates or as interconnected acicular structures. The α -AlFeMnSi phases with a Chinese script morphology and β - Al_5FeSi platelets were also seen in the base alloy (Fig.1a) but less frequently. The Si particles appear both as primary blocky particles and as acicular eutectic particles. The 3D morphology of the β - Al_5FeSi phase and especially the Al_9FeNi (Fig. 1b) particle is clearly exposed by porosity.

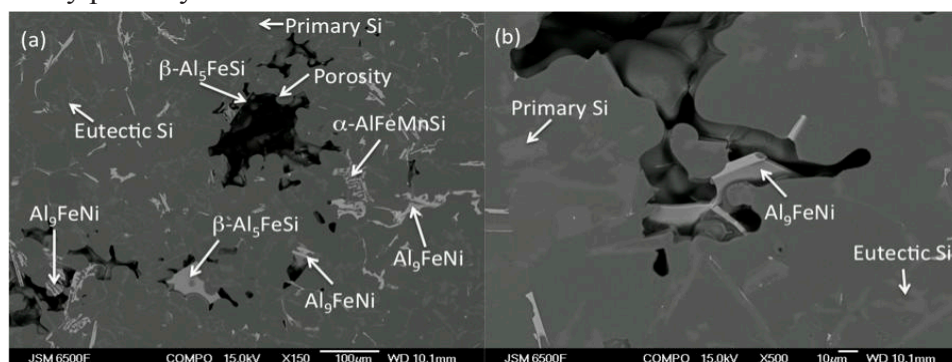


Fig. 1 (a) A typical SEM micrograph of the base alloy showing various intermetallics with some interconnected with porosity. (b) A SEM image showing a Al_9FeNi particle inside a pore.

In the 0.02%Sr and 0.05%Sr modified alloys, there are no primary Si particles and the eutectic Si appears as a well modified fibrous structure as shown in Fig. 2. However, Sr led to segregated regions of intermetallics in which the Si particles were partially modified. Phases observed included Al_9FeNi , Mg_2Si , λ - $\text{Al}_5\text{Cu}_2\text{Mg}_8\text{Si}_6$, $\text{Al}_3(\text{CuNi})_2$ and the α -AlFeMnSi phase which also contained Cr, Ni and Cu (Fig. 2c). Fewer β phases were observed in the 0.02%Sr alloy compared to the base alloy but none was observed in the 0.05%Sr alloy providing further confirmation of the suppression of this phase via

Sr addition. In general, the intermetallics in the 0.05%Sr appeared more refined and mostly script-like. Note the 3D morphology of the λ -phase (Fig. 2c) exposed by porosity. This observation and that in Fig. 1 underscores the significance of all types of intermetallics in pore formation and not just the β -phase. No β -phases were observed in the 0.02%Sr+0.53%Mn alloy but large acicular and plate-like Al_9FeNi phases were observed with other intermetallics such as $\text{Al}_3(\text{NiCu})_2$, Mg_2Si , Al_2Cu , $\lambda\text{-Al}_5\text{Cu}_2\text{Mg}_8\text{Si}_6$ and Chinese script $\alpha\text{-AlFeMnSi}$ phases.

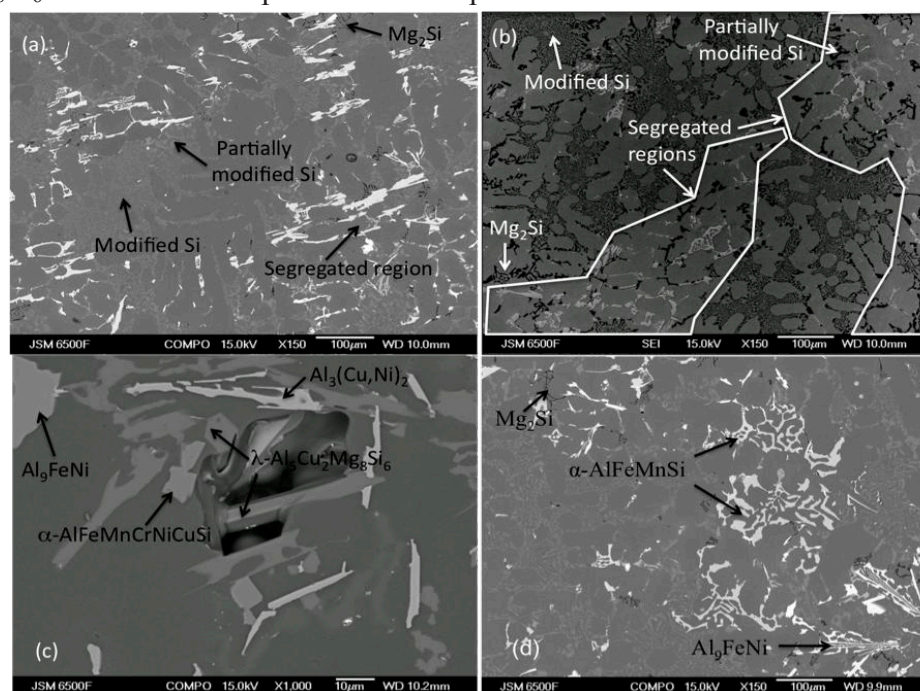


Fig. 2 SEM micrographs of (a) 0.02%Sr alloy and (b) 0.05%Sr (SEI) showing segregated regions with intermetallics and partially modified Si particles and regions of fully modified Si, (c) 0.05%Sr alloy showing intermetallics in 3D inside porosity and (d) 0.02%Sr+0.53%Mn alloy.

The microstructure of the 0.02%Sr+0.28%Al-5Ti-1B alloy was similar to that of 0.02%Sr alloy except for the occasional large β -phases as shown in Fig. 3a. Numerous β -phases were observed in the 0.2%Sb alloy (Fig. 3b & 3c). This is, to the authors' knowledge, unique and may be attributed to a possible increased nucleation of β -phases on Sb-bearing phases that were also observed in the microstructure. Phosphorus is reported to increase β -phases due to their increased nucleation on AIP particles [13]. Since β and Si particles both nucleate on AIP [14] and the fact that Sb refines Si particles [6,15], it is reasonable to suggest that Sb can affect β -phase formation in the same manner. Further evidence is however required to confirm this hypothesis. Other phases were also observed in this alloy including Al_9FeNi , $\text{Al}_3(\text{NiCu})_2$, Mg_2Si , $\lambda\text{-Al}_5\text{Cu}_2\text{Mg}_8\text{Si}_6$ and $\pi\text{-Al}_8\text{FeMg}_3\text{Si}_6$. The β -phases disappear with further addition of 0.53%Mn to the 0.2%Sb alloy. However, Al_9FeNi phases appeared both as thin and thick platelets as well as connected acicular structures, while the $\alpha\text{-AlFeMnCrSi}$ phases appeared as compact particles and as large skeleton structures (Fig. 3d).

Addition of 0.05%Sr+0.53%Mn resulted in extensive networks of $\alpha\text{-AlFeMnCrSi}$ phases that appeared as neatly lined compact particles (see Fig. 4a). These particles are however connected in 3D as observed in CT slices and inside pores. Also observed were $\text{Al}_3(\text{NiCu})_2$, Mg_2Si and $\lambda\text{-Al}_5\text{Cu}_2\text{Mg}_8\text{Si}_6$ particles. Fig. 4b shows compact $\alpha\text{-AlFeMnCrSi}$ and Al_9FeNi particles in the 1%Cr alloy. These phases were also seen in the 0.53%Mn alloy but the $\alpha\text{-AlFeMnCrSi}$ phase was skeleton shaped (Fig. 4c). $\text{Al}_3(\text{NiCu})_2$ and Mg_2Si phases were also observed. Star-shaped and compact script-like $\alpha\text{-AlFeMnCrSi}$ particles were seen in the 0.3%Mn+0.2%Cr alloy (Fig. 4d).

Table 1 shows a summary of the quantitative measurements of porosity and intermetallic characteristics in the alloys. Sizes of the largest pores and intermetallics were measured in terms of

their maximum feret dimension (L_f) and the equivalent circle diameter (D_{eq}). The area fraction (A_f) of intermetallics was also measured from 2D images for comparison with V_f . There is no apparent correlation between V_f , A_f , L_f , D_{eq} , and α but the results show that the largest pores or intermetallics have low aspect ratios implying that they are irregularly shaped. This observation was valid even in Sr-modified alloys in which large pores with aspect ratios of around 0.8 were observed as shown in Fig. 5. The V_f of intermetallics increased with element addition except for 0.2%Sb alloy in which it reduced. This reduction may be associated with the preferential β -phase formation.

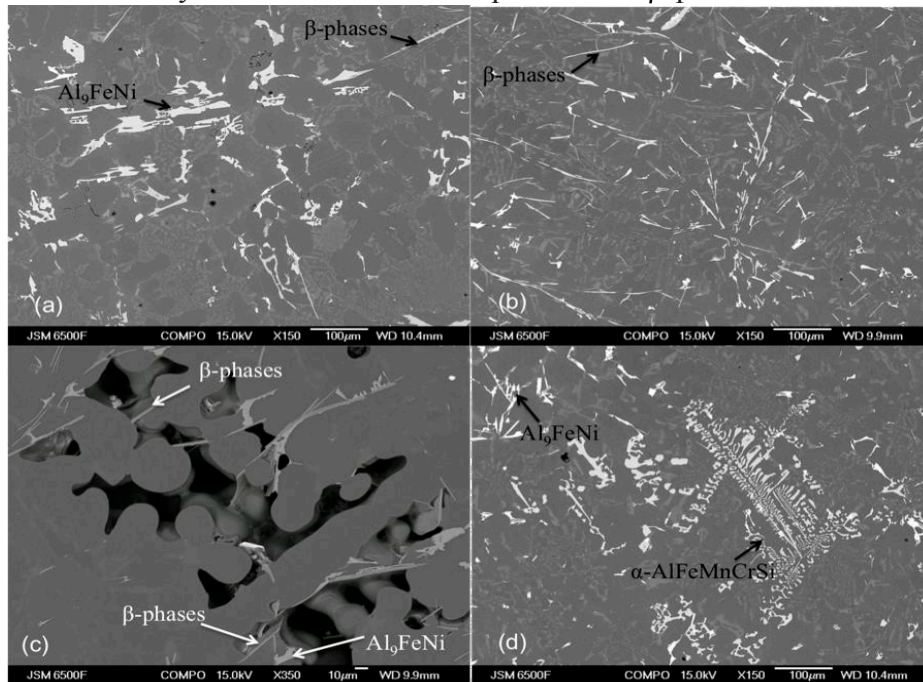


Fig. 3 SEM micrographs of (a) 0.02%Sr+0.28%Al-5Ti-1B alloy, (b) 0.2%Sb alloy showing several β -phases, (c) 0.2%Sb showing β -phases associated with pores and (d) 0.2%Sb+0.53%Mn showing a large skeleton α -AlFeMnCrSi phase.

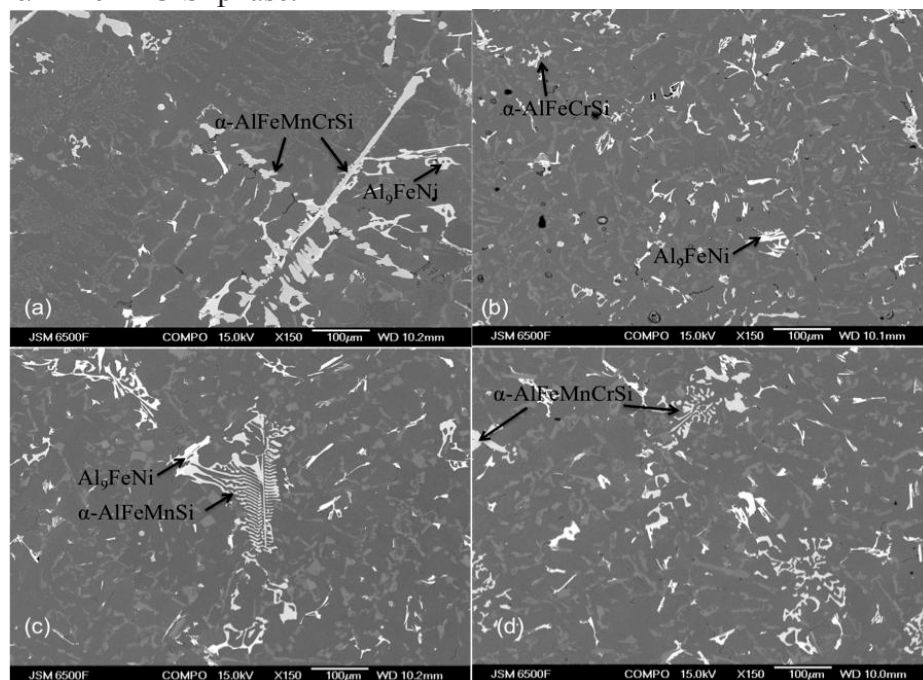


Fig. 4 SEM micrographs of (a) 0.05%Sr+0.53%Mn alloy showing a large α -AlFeMnCrSi phase, (b) 1%Cr alloy showing fine and compact phases, (c) 0.53%Mn with a large skeleton α -AlFeMnSi phase and (d) 0.3%Mn+0.2%Cr alloy with star and script-like α -AlFeMnCrSi.

Table 1 further shows that the level of porosity (V_f) is higher in the 0.02%Sr alloy (1.5%) compared to the 0.05%Sr alloy (1.25%). This can be attributed to finer intermetallics and absence of the β phases in the 0.05%Sr. A large maximum pore size is also observed in the 0.02%Sr alloy ($L_f=993 \mu\text{m}$) which is only comparable to those in 0.02%Sr+0.28%Al-5Ti-1B ($L_f=991 \mu\text{m}$) and 0.05%Sr+0.53%Mn ($L_f=895 \mu\text{m}$) alloys. Both 0.02%Sr and 0.05%Sr alloys however have higher porosity levels than the base alloy (0.03%). The pores in these alloys were both in spherical form as well as irregularly shaped as shown in Fig. 5. The irregular shaped pores were always connected with intermetallics indicating that they are shrinkage pores formed due to feeding difficulties occasioned by the intermetallics. The spherical pores on the other hand were generally not linked to intermetallics but surrounded by a modified eutectic. These may be attributed to their early nucleation which is facilitated by Sr addition through various mechanisms including a reduction in the surface tension of the melt [15]. The transformation of the eutectic nucleation and solidification mode due to chemical modification has also been shown to affect pore formation characteristics [16].

Table 1 Quantitative measurements of porosity and intermetallic characteristics in the various alloys

<i>Pores</i>	P	P2Sr	P5Sr	PSb	PMn	PCr	PMnCr	P2SrGr	P2SrMn	P5SrMn	PSbMn
V_f %	0.03	1.5	1.25	0.13	0.04	<0.01	0.04	1.21	0.38	1.33	0.48
Max. L_f	427	923	374	499	276	90	273	991	428	895	837
D_{eq}	185	390	143	197	89	37	131	528	224	416	104
α	0.103	0.056	0.083	0.057	0.181	0.238	0.334	0.132	0.273	0.056	0.166
<i>phases</i>											
V_f %	10	13.2	12.6	9.3	13.7	14.9	13.5	12.8	14.2	15.7	13.3
A_f %	4.14	4.96	5.15	6.9	5.7	5.47	6.03	5.4	7.3	9.3	6.97
L_f	248	163	212	280	338	116	342	277	401	707	294
D_{eq}	76	52	76	82	84	52	91	104	71	94	99
α	0.008	0.12	0.028	0.032	0.006	0.122	0.008	0.008	0.008	0.022	0.011

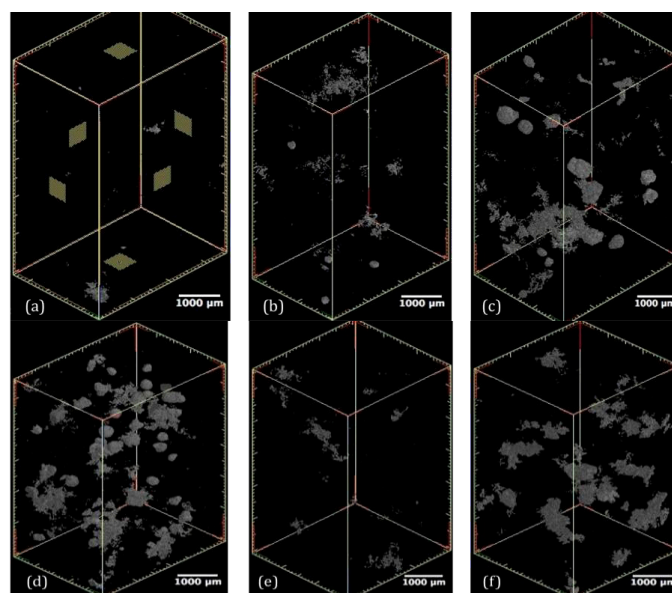


Fig. 6 Representative 3D μCT images showing porosity distribution in the (a) base alloy, (b) 0.05%Sr, (c) 0.02%Sr, (d) 0.02%Sr+0.28%Al5TiB, (e) 0.02%Sr+0.53%Mn and (f) 0.05% Sr+0.53% Mn alloys.

The increase in β -phases may explain the increase in porosity in the 0.2%Sb alloy compared to the base alloy contrary to previous reports [6,15]. It has been previously proposed that one of the mechanisms leading to increased porosity due β -phases is the competition for nucleant particles between eutectic grains and the β particles [14]. It is suggested that this leads to an increase in the size

of eutectic grains that eventually obstruct liquid feed paths [14]. Further addition of 0.53%Mn to the 0.2%Sb alloy leads to a disappearance of β -phases and 64% reduction in porosity. However, the presence of large intermetallics can obstruct feed paths and may explain the higher level of porosity in the 0.2%Sb+0.53%Mn alloy compared to the base alloy.

The 1%Cr alloy recorded the lowest porosity level with $V_f < 0.01\%$, followed by the 0.53%Mn and 0.3%Mn+0.2Cr alloys with $V_f=0.04\%$ each. The low level of porosity is attributed to the compact nature of the intermetallics observed in these three alloys. The Sr modified alloys registered the highest porosity levels except for the 0.02%Sr+0.53%Mn alloy in which the addition of 0.53%Mn led to a 75% reduction in porosity in the 0.02%Sr modified alloy. The reduction in porosity in this alloy may be associated with a reduction of eutectic grain sizes due to Mn addition which in turn increases the mobility of feed liquid [14]. This is supported by the absence of spherical pores in this alloy (see Fig. 5e). The 0.05%Sr+0.53%Mn alloy however has a higher level of porosity (1.33%) than its 0.05%Sr counterpart. Spherical pores were also not observed in this alloy but massive shrinkage pores were seen associated with intermetallics. This alloy has massive networks of α -AlFeMnCrSi intermetallics throughout the microstructure. Addition of 0.28%Al-5Ti-1B grain refiner to the 0.02%Sr alloy slightly reduced porosity by 19% but the overall pore characteristics did not change.

4. Conclusion

The influence of individual and combined additions of Sr, Sb, Mn, Cr and Al-5Ti-1B grain refiner on the microstructure and porosity characteristics of a secondary Al-Si piston alloy was investigated. Results show that the volume fraction (V_f) of intermetallics increased with minor element additions except when 0.2%Sb was added. Sb decreased V_f but increased β -Al₅FeSi particles in the alloy. This effect was cancelled with addition of 0.2%Sb+0.53%Mn. Porosity increased with all additions except for 1%Cr, which resulted in fine compact intermetallics and reduced porosity. Addition of 0.53%Mn and 0.3%Mn+0.2%Cr also resulted in compact phases and low porosity. Porosity was highest in the Sr-modified alloys with 0.02%Sr giving higher porosity than 0.05%Sr. However, porosity reduced in the 0.02%Sr alloy with 0.53%Mn addition while addition of 0.53%Mn+0.05%Sr significantly increased the level of porosity and intermetallics.

References

- [1] P.N. Crepeau: AFS Trans. 103 (1995) 361-366.
- [2] T. O. Mbuya, B. O Odera and S. P. Ng'ang'a: Int. J. Cast Met. Res. 16 (5) (2003) 451-465.
- [3] J.Y. Hwang, H.W. Doty and M. J. Kaufman: Mater. Sci. Eng. A, 488 (2008) 496-504.
- [4] G. Gustafsson, T. Thorvaldsson and G. L Dunlop: Metall. Trans. A. 17A (1986) 45-52.
- [5] H.Y. Kim, W. H. Sang and H. M Lee: Mater. Lett. 60 (2006) 1880-1883.
- [6] M. Garat, G. Laslaz, S. Jacob, P. Meyer and R. Adam: AFS Trans., 100 (1992) 821-832.
- [7] S.G. Shabestari, M. Mahmud, M. Emamy & J. Campbell: Int. J. Cast Met. Res. 15 (2002) 17-24.
- [8] A.M. Samuel, F.H. Samuel and H.W. Doty: J. Mater. Sci. 31 (1996) 5529-5539.
- [9] C.R.S. Daykin: *Microstructural Modelling of Commercial Aluminium-Silicon Alloys for Piston Applications*, PhD Thesis, University of Cambridge, 1998.
- [10] Z. Qian, X. Liu, D. Zhao and G. Zhang, Mater. Lett., 62 (2008) 2146-2149.
- [11] C.L. Chen, G. West and R.C. Thomson: Mater. Sci. Forum, 519-521 (2006) 359-364.
- [12] C.L. Chen, *Characterisation of Intermetallic Phases in Multicomponent Al-Si Alloys for Piston Applications*, PhD Thesis, IPTME, Loughborough University, 2006.
- [13] A.M. Samuel, F.H. Samuel, C. Villeneuve, H. Doty and S. Valtierra: Int. J. Cast Metals res., 14 (2001) 97-120.
- [14] C.M. Dinnis, J.A. Taylor and A.K. Dahle: Metall. Mater. Trans. A, 37A (2006) 3283-2191.
- [15] R. Fuoco, E.R. Correa and A.V.O. Correa: AFS Trans., 103 (1995) 379-387.
- [16] L. Lu, K. Nogita, S.D. McDonald and A.K. Dahle: JOM, Nov. (2004) 52-58.